Synthesis, Characterization and Remarkable Anticancer Activity of Rhenium Complexes Containing Biphenyl Appended NNN Donor Sulfonamide Ligands

Chiranthi Kaushalya[1], Taniya Darshani[1], Sameera R Samarakoon[2], Frank R Fronczek[3], Inoka C Perera[4] and Theshini Perera[*1]

[1]Department of Chemistry, University of Sri Jayewardenepura, Sri Lanka.

[2]Institute of Biochemistry, Molecular Biology and Biotechnology, University of Colombo, Sri Lanka

[3]Department of Chemistry, Louisiana State University, Baton Rouge, Louisiana, USA.

[4]Department of Zoology and Environment Science, University of Colombo, Sri Lanka.

Abstract

Neutral and cationic rhenium complexes provide both hydrophilic as well as hydrophobic properties due to the robustness of the tridentate ligand system of biphenyl appended dipicolylamine (N(SO$_2$bip)dpa) and diethylenetriamine (N(SO$_2$bip)dienH) coordinated to the [Re(CO)$_3$]$^+$ core, hold immense potential for the development of metal based anticancer drugs. This was achieved by the synthesis of two ligands (L1: N(SO$_2$bip)dpa and L2: (N(SO$_2$bip)dienH) and their corresponding Re complexes (C1: [Re(CO)$_3$(N(SO$_2$bip)dpa)]PF$_6$ and C2: [Re(CO)$_3$(N(SO$_2$bip)dien)] in good yield and high purity. All four compounds were characterized by ^{1}H NMR, UV-Vis, FTIR spectroscopies and L1, also by single crystal X-ray diffraction. The methylene protons observed as a singlet at (4.59 ppm) in a ^{1}H NMR spectrum of L1 appear as two doublets (5.66 and 4.65 ppm) in the spectrum of C1. The appearance of NH signals at 3.48, 5.17 and 6.69 ppm in the ^{1}H NMR spectrum of C2 confirm the coordination of L2 with Re. The stretching vibration frequencies depicted by the S-N bond at 923 cm^{-1} for L1 appear towards lower frequencies (821 cm^{-1}) in an FTIR spectrum of C1, while the S-N bond at 943 cm^{-1} for L2 appears towards higher frequencies (968 cm^{-1}) in C2. *In silico* assessment of drug likeliness revealed zero violations demonstrating a high likeliness of the ligands to be successful as drug leads. All four compounds have shown very low IC$_{50}$ values against non-small cell lung cancer cells (NCI-H292). Therefore, L1, C1, L2 and C2 are promising novel compounds that can be further investigated as potential anticancer agents.

Keywords: Rhenium Tricarbonyl, Sulfonamide, Anticancer, Fluorescence.

1. Introduction

A significant part of drug discovery in the last forty years has focused on agents to prevent or treat cancer (Garcia, Jemal et al. 2007, Kunnumakkara, Bordoloi et al. 2019). While the development of modern medicinal chemistry for cancer treatment was stimulated by the serendipitous discovery of cisplatin, [*cis*-PtCl$_2$(NH$_3$)$_2$] (Cleare and Hoeschele 1973), rhenium(I) complexes have attracted the attention of medicinal

chemists (Schibli and Schubiger 2002). These metal complexes are kinetically inert; thus, ligand substitution is avoided when the coordination spheres are formed by suitable ligand systems (Schibli, Schwarzbach et al. 2002). On the other hand, good fluorescent probes have been prepared by utilizing rhenium(I) complexes to study the cell behavior *in vitro* (Lo, Louie et al. 2008, Lo, Zhang et al. 2011, KK-W, AW-T et al. 2012, KK-W. 2015) because of useful properties, including long lifetime and large Stokes shifts exhibited by rhenium (Christoforou, Marzilli et al. 2007). An outstanding solubility in aerobic aqueous solutions has been exhibited by rhenium(I) complexes, leading them to be chosen for biological applications (Schibli and Schubiger 2002, Desbouis, Struthers et al. 2008). The organometallic, semi aqua, ionic complex with general formula $[M(H_2O)_3(CO)_3]^+$ (M: Re, Tc) has gained extensive use since the development of a kit preparation by Alberto and co-workers (Schibli and Schubiger 2002). There are three coordinative sites available for ligand substitution in $[M(H_2O)_3(CO)_3]^+$ complex, and regardless of softness and hardness, mono, bi, and tridentate ligand systems can be incorporated into the tricarbonyl core (Christoforou, Marzilli et al. 2007) delivering remarkable chemical and biological features which are applicable in imaging and therapeutic applications (Amoroso, Coogan et al. 2007).

Three main conceptual steps have been recognized in the interaction of a drug with a biological system; penetration, binding and action (Testa, Crivori et al. 2000). The selection of the ligand should be done carefully as the lipophilic nature of the ligand may improve the ability of a chemical compound to dissolve in fats, oils and lipids as well as contribute towards the overall lipophilicity of the metal complex (Testa, Crivori et al. 2000, Arnott and Planey 2012, Rutkowska, Pajak et al. 2012) Thus, in designing suitable ligands for our study, we paid attention on obtaining amphipathic ligands expecting better cellular uptake. Furthermore, the ligand systems were selected as having predicted affinities to cellular receptors expecting selective uptake.

Our attention was caught by biphenyl which is an aromatic hydrocarbon having a molecular formula of $(C_6H_5)_2$ which has displayed remarkable properties in early studies (Wolf, O'Kelly et al. 2007, Pizarro and Sadler 2009). Honokiol (HNK) is a naturally occurring biphenyl which has exhibited potent anti-proliferative activity against breast cancer cell lines and enhanced the activity of other drugs used for the treatment of breast cancer; but also has long been known to have anti-thrombosis, antibacterial and anxiolytic effects (Wolf, O'Kelly et al. 2007). A biphenyl coordinated ruthenium complex has been shown to display promising anticancer activity; NMR studies have revealed that the biphenyl analogue, $[(\eta^6\text{-}bip)Ru(en)Cl]^+$ binds DNA through a combination of both coordination bonds and non-covalent interactions (Pizarro and Sadler 2009). Thus, as a result of the extended π electron system in the biphenyl ligand, non-coordinative hydrophobic interactions between the biphenyl and DNA can occur (Atkins, Overton et al. 2006, Pizarro and Sadler 2009). Furthermore, DNA binding studies of osmium complexes have revealed that the coordination with DNA strands is mainly due to non-coordinative interactions of biphenyl and ethylene diammine ligands (Atkins, Overton et al. 2006, Pizarro and Sadler 2009). Hence in this study, biphenyl has been selected as a candidate to be used as a component in a ligand system expected to be lipophilic, resulting in possible bio recognition and intercalation with DNA to gain promising anticancer activity in the ligand system and its metal complex. We also took into consideration the fact that anticancer (Scozzafava, Owa et al. 2003) and antimicrobial activities (Kadi, El-Brollosy et al. 2007) have been displayed by sulfonamide derivatives. The replacement of amine proton of *N*(H)dpa by various substituents such as RSO_2Cl, facilitates the formation of C-N bond in *N*(SO_2R)dpa ligands, leading to the eventual synthesis of *fac*-$[Re(CO)_3(N(SO_2R)dpa)]^+$ complexes, having useful biochemical properties (Perera, Abhayawardhana et al. 2013).

Re(I) complexes synthesized with *N*(SO_2R)dienH ligands have also shown promising chemical characteristics (Abhayawardhana, Marzilli et al. 2014) and may possess enhanced biological activity. These ligands are composed of hydrophilic $-CH_2NH_2$ groups and have the advantage of being small in size. For the development of small nuclide radiopharmaceuticals, a neutral metal containing label is the

104

most useful because neutral labels are most likely to preserve the biological properties of lagged species. A net neutral coordination unit can be best achieved with a *fac*-M(CO)$_3^+$ core (M = Tc, Re) with a facially coordinated monoanionic tridentate ligand. This can be fulfilled by treating *fac*-[Re(CO)$_3$(H$_2$O)$_2$]$^+$ with an unsymmetrical NNN donor ligand-based primarily on diethylenetriamine (dien) moiety with an aromatic group linked to terminal nitrogen through a sulfonamide (Christoforou, Marzilli et al. 2007).

The main objective of this study was to integrate biphenyl derivatied ligands into rhenium tricarbonyl complexes as a potential bio tool to recognize and treat cancerous cells in the human body. The *N*(SO$_2$bip)dpa (L1) and *N*(SO$_2$bip)dienH (L2) ligands were used as a means to incorporate the biphenyl group via a sulfonamide linkage to the well-known dipicolylamine and diethylenetriamine moieties, respectively. Thereby, newly synthesized Re-N bonded complexes (Figure 1), as well as the ligands, were assessed for their potential applicability as anticancer agents.

2. Experimental section
2.1. Starting materials

Re$_2$(CO)$_{10}$, AgOTf,biphenyl-1-sulfonyl chloride, di-(2-picolyl)amine(N(H)dpa), diethylenetriamine, NaPF$_6$, anhydrous sodium sulphate, acetone, methanol, dichloromethane, chromasolv water and dioxane were obtained from Sigma Aldrich, USA. NCI-H292 (non-small cell lung cancer cells) was obtained from American Type Culture Collection. All the solvents and chemicals were of analytical grade and were used as received without further purification.

2.2. Methodology

^{1}H NMR spectra were recorded in DMSO-d_6 on a Bruker 400 MHz spectrometer. Peak positions are relative to tetramethylsilane (TMS) as reference. All NMR data were processed with MestReNova software. Single crystals of L1 were placed in a cooled nitrogen gas stream at 90 K on a Bruker Kappa Apex-II DUO diffractometer equipped with Mo *Kα* radiation (λ = 0.71073 Å). Refinement was performed by full-matrix least squares methods using SHELXL(Fulmer, Miller et al. 2010) with H atoms in idealized positions. Molecular graphics are drawn using *ORTEP-3* for windows.(Banerjee, Levadala et al. 2002) Electronic spectra for ligands and metal complexes were obtained on Spectro UV-Vis auto version 3.10, UV-2602 spectrophotometer. The spectral range was 190 nm-1100 nm. Spectra were obtained in methanol with baseline correction. Spectral data were processed with UV WIN software. FTIR spectra were recorded on a Thermo scientific NICOLET iS10 spectrophotometer. ATR spectra were obtained within the 4000-600 cm^{-1} spectral range. Spectral data were processed with OMNIC software. Emission spectra were obtained in methanol on a Thermo scientific Lumina spectrophotometer. A 150 W Xenon lamp was used as the excitation source. Spectral data were processed with Luminous software.

2.3. Synthesis

By using Re$_2$(CO)$_{10}$, [Re(CO)$_3$(H$_2$O)$_3$]OTf was prepared as the starting material according to a known procedure(He, Lipowska et al. 2005) to enable the synthesis of the metal complexes.

2.3.1. N(SO2bip)dpa ligand (L1)

L1 was synthesized according to a known procedure (Vitharana, Kaushalya et al.) A solution of

105

biphenyl-4-sulfonyl chloride (5 mmol) in 25 ml of dioxane was added dropwise over 2 h to a solution of $N(H)$dpa (10 mmol) in 100 ml of dioxane at 20 °C, and the mixture was stirred for 24 h at room temperature. It was filtered to remove any precipitate, and dioxane was removed by rotary evaporation. Weakly acidic water (30 ml, pH~5) was added to the resulting compound, and the product was then extracted into CH_2Cl_2 (2x25 ml); the CH_2Cl_2 extracts were combined and taken to dryness to give a brown-coloured solid. The ^1H NMR data and UV visible data matched reported values. Anal. Calcd for $C_{24}H_{21}N_3SO_2$ (%): C, 68.63; H, 05.01; N, 10.44; S, 7.97. Found: C, 67.76; H, 05.21; N, 10.16; S, 7.68. Slow evaporation from a solution of the compound in methanol yielded crystals suitable for single crystal X-ray diffraction.

2.3.2. N([Re(CO)₃(N(SO₂bip)dpa)]PF₆ (C1)

A solution of N(SO$_2$bip)dpa (0.1 mmol) in 2.00 ml water and 3.00 ml methanol was treated with aqueous [Re(CO)$_3$(H$_2$O)$_3$]OTf (0.1 mmol, 1.00 ml). Methanol (3.00 mmol) and water (1.00 ml) were added to dissolve the precipitate formed. Acidity of the solution was measured (pH~5). The clear solution was heated at reflux overnight. A slight excess of NaPF$_6$ was added to the clear solution, and the resultant precipitate was filtered using normal filter paper. The precipitate was allowed to dry. The dried precipitate was re-dissolved by adding a minimum amount of acetone and subjected to slow evaporation of the solvent to give a light cream colour solid (0.068g, 82%). NMR signals (ppm) in DMSO-d_6: 8.89 (2H, H6/H6'), 8.41 (d, 2H, Ha/Ha'), 8.24 (d, 2H, Hb/Hb'), 8.03 (t, 2H, H4/H4'), 7.92 (d, 2H, Hc/Hc'), 7.54-7.63 (m, 3H, Hd/Hd' and He), 7.46-7.51 (m, 4H, H3/H3' and H5/H5'), 5.66 (d, 2H, *endo*-H), 4.65 (d, 2H, *exo*-H).

2.3.3. N(SO₂bip)dienH (L2)

A solution of biphenyl-4-sulphonyl chloride (5 mmol) in 100 ml of dioxane was added dropwise over 2 h to a solution of N(H)dien (50 mmol) in 100 ml of dioxane. The reaction mixture was stirred overnight at room temperature. The dioxane was completely removed under a vacuum and water (50 ml) was added. The product was extracted into CH_2Cl_2 (2x100 ml), and the solvent was removed under rotary evaporation. A pale yellow-coloured, oily precipitate was obtained (1.549 g, 97%). Anal. calc. for $C_{16}H_{21}N_3O_2S.2H_2O$: C, 54.06, H, 7.09, N, 11.82, S, 9.02. Found: C, 55.27, H, 6.41, N, 11.02, S, 8.82%. NMR signals (ppm) in DMSO-d_6: 7.86-7.89 (m, 4H, Ha/Ha' and Hb/Hb'), 7.71-7.75 (m, 2H, Hc/Hc'), 7.42-7.53 (m, 3H, Hd/Hd' and He), 2.39-2.87 (m, 8H).

2.3.4. [Re(CO)₃(N(SO₂bip)dien)] (C2)

A solution of [Re(CO)$_3$(H$_2$O)$_3$]OTf (0.1 mmol) in 10 ml of water was treated with a solution of ligand (0.1 mmol) dissolved in 5 ml of methanol. The pH was adjusted to ~5, and then the reaction mixture was heated at reflux for 16 h and allowed to cool at room temperature, and the pH was increased to ~7. The white-coloured precipitate which was obtained was filtered (0.032g, 54%). NMR signals (ppm) in DMSO-d_6: 7.83 (d, 2H, Ha/Ha'), 7.77 (d, 2H, Hb/Hb'), 7.72 (t, 2H, Hc/Hc'), 7.47-7.50 (m, 3H, Hd/Hd' and He), 6.69 (s, 1H), 5.15-5.17 (1H), 3.48 (s, 1H), 2.64-2.90 (m, 8H).

2.4. Biological Studies

2.4.1. Prediction of drug-likeness

Scoring servers based on Lipinski's "rule of five" was used to predict the drug-likeness of the ligands L1 and L2. The molecular properties such as molecular weight (MW), the logarithm of the octanol/water partition coefficient (LogP), hydrogen bond donors (HBD), hydrogen bond acceptors

(HBA), topological polar surface area (TPSA) and rotatable bonds were used as the parameters to deduce the drug-likeness of the ligands. The properties were calculated by computational studies such as molinspiration (www.molinspiration.com), ChemAxon (www.chemicalize.org) and molsoft (https://www.molsoft.com) servers.

2.4.2. In vitro cytotoxic effects

Non-small cell lung cancer cells (NCI-H292) cells were plated on 96 well plates (5000 cells/well) with Dulbecco's Modified Eagle Medium (DMEM; Sigma Aldrich D5648) supplemented with 10% Fetal Bovine Serum (FBS) and incubated at 37 °C under 5% CO_2 for 24 h. Cells were exposed to test compounds (concentrations ranging from 25 to 400 μg/mL) for 24, 48 and 72 h. Cytotoxicity was assessed by Sulforhodamine B assay. The absorbance values were measured at 540 nm, and the results were expressed as percentage cell viability. The percentage cell viability was calculated by the equation given below. Data were normalized and analyzed IC_{50} values were calculated using log concentration vs normalized absorbance percentage curves by GraphPad Prism 6.0.1.

$$\text{Viable cell (\%)} = \frac{\text{Absorbance of treated cells}}{\text{Absorbance of untreated cells}} \times 100$$

3. Results and Discussion

Two tridentate ligands bearing a biphenyl group incorporated via a sulfonamide linkage at the central nitrogen of *N*(H)dpa and one terminal nitrogen of *N*(H)dien were synthesized in good yield by coupling them with bipSO$_2$Cl (Figure 1). Although the synthesis of L1 has been reported (Vitharana, Kaushalya et al.), we report here for the first time the single crystal structure of L1. The reaction of synthesized ligands (*N*(SO$_2$bip)dpa (L1) and *N*(SO$_2$bip)dienH (L2) with an aqueous solution of [Re(CO)$_3$(H$_2$O)$_2$]OTf afforded [Re(CO)$_3$(*N*(SO$_2$bip)dpa)]PF$_6$ (C1) and [Re(CO)$_3$(*N*(SO$_2$bip)dien)] (C2) complexes, respectively.
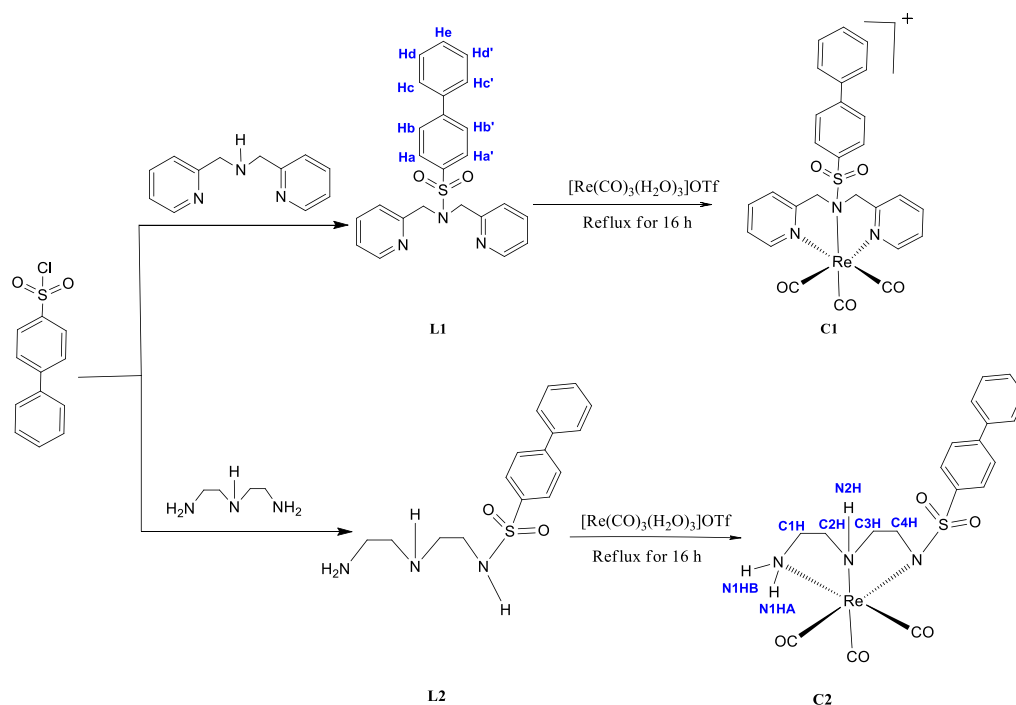

Figure 1. Schematic diagram of the reaction pathways involved in the synthesis of ligands and metal complexes.

3.1. Characterization

3.1.1. NMR Spectroscopy

Compounds reported in this study were characterized by ^{1}H NMR spectroscopy in DMSO-d_6 at 298 K. All the peaks were assigned related to the structure of both ligand and metal complex, based on the chemical shifts, coupling constants, splitting patterns as well as the integrations of corresponding peaks. The ^{1}H NMR spectrum of N(SO$_2$bip)dpa (L1) matched reported values (Vitharana, Kaushalya et al.).

It is evident from a ^{1}H NMR spectrum of [Re(CO)$_3$(N(SO$_2$bip)dpa]PF$_6$ (C1) that the methylene protons of L1 have acquired a new arrangement (Figure 2) upon coordination of the ligand with rhenium, becoming magnetically dissimilar. The magnetically distinct protons in –CH$_2$ are designated as *endo*–H or *exo*-H on the basis of the orientation of protons either towards (*endo*) or away (*exo*) from carbonyl ligands. Hence, methylene protons in C1 complex give rise to two doublets (5.66 and 4.65 ppm) and are shifted downfield in comparison with the methylene protons of L1 (Figure 2).
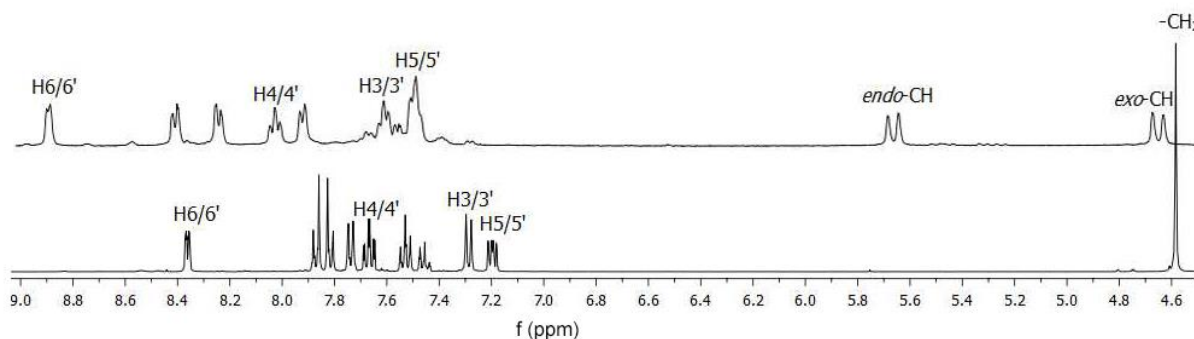
Figure 2. ^{1}H NMR spectra of N(SO$_2$bip)dpa (bottom) and [Re(CO)$_3$(N(SO$_2$bip)dpa]PF$_6$ (top) in DMSO-d_6.

Significant downfield chemical shifts are observed for all the signals attributed to the inequivalent protons present in the ligand upon coordination, providing strong evidence for the formation of the metal complex. These downfield chemical shifts are caused by the inductive effect resulting from the direct Re–N bond (Subasinghe 2015). It is noteworthy that the downfield shifts are determined by the close proximity of protons to the pyridyl nitrogen for pyridyl protons, whereas for biphenyl protons, it is decided by the distance of the proton and central nitrogen that coordinates with Re. Therefore, the downfield shift increases with the decrease of the number of bonds between H(pyridyl) and N(pyridyl) or H(biphenyl) and N(sulfonamide).

In ^{1}H NMR spectra recorded for N(SO$_2$bip)dienH (L2) recorded in DMSO-d_6 at 298 K, although the biphenyl group possesses five magnetically inequivalent protons, only four peaks can be clearly observable in the range of 7.00-8.00 ppm in the aromatic (Figure 3). The value for integration of the peak positioned at 7.89-7.86 ppm reveals that it is due to two signals of magnetically inequivalent protons, which can be assigned as Ha/a' and Hb/b'. The peak positions for the protons in the biphenyl group of a spectrum of L1 are very much similar to that of L2. The other zone, which is situated more upfield on the spectrum contains the signals of methylene protons of dien backbone. Out of the four chemically inequivalent protons, the protons attached to the carbon, located adjacent to sulfonamide nitrogen (C4H) are the most deshielded due to the close proximity to both nitrogen and sulfonamide oxygen. Hence C4H is placed more downfield on the spectrum, followed by the triplets of other methylene carbons (C3H, C2H and C1H). The singlets related to solvent residual peaks are also positioned upfield in close proximity to the signals of methylene protons at 3.14, 3.26, 3.57 and 2.50 ppm for methanol, D$_2$O, dioxane and DMSO, respectively.
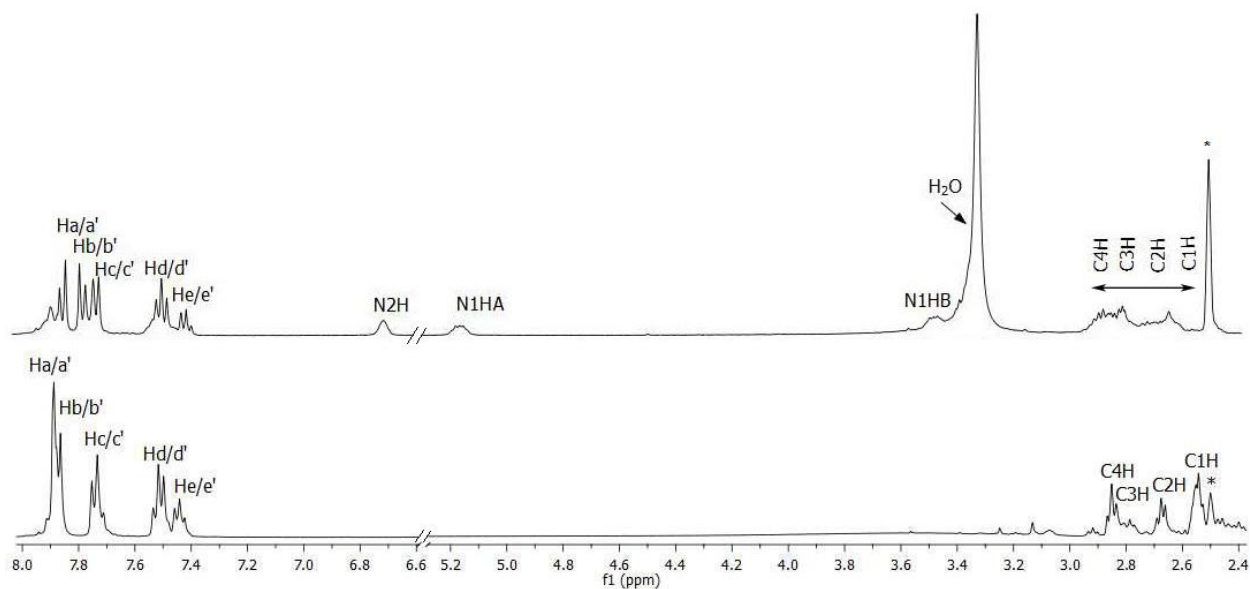
Figure 3. The ^{1}H NMR spectra of N(SO$_2$bip)dienH (bottom) and [Re(CO)$_3$(N(SO$_2$bip)dien)] (top) in DMSO-d_6.

Signals associated with biphenyl protons appear more upfield in C2 (Figure 3) in comparison to that of L2, possibly due to stacking effects of the biphenyl moiety. Upon coordination, the proton on the sulfonamide nitrogen deprotonates, and the neutral ligand is converted to an anion, which in turn neutralizes the +1 charge on Re. Therefore, a neutral metal complex has been formed.

The appearance of three singlets at 3.48 ppm, 5.17 ppm, and 6.69 ppm (Figure 3) in the ^{1}H NMR spectrum of C2, related respectively to N1HB, N1HA and N2H, which were absent in the free ligand spectrum, are further proof of metal complex formation. The protons of the terminal –NH$_2$ group have become magnetically inequivalent due to the *endo* and *exo* phenomenon that was described previously by Christoforou *et al.* and the positions of –NH protons on the ^{1}H NMR spectrum of C2 are very much similar to that of Re(CO)$_3$(tmbSO$_2$-dien) described therein (Christoforou, Marzilli et al. 2007). The peaks at 3.33 ppm and 2.50 ppm are attributed to solvent residual peaks.

3.1.2. Structural results

Crystals of N(SO$_2$bip)dpa (L1) were obtained in methanol, and single crystal diffraction data were collected and deposited with the Cambridge Crystallographic Data Centre under deposition number CCDC 1855997. Crystal data and structure refinement for L1 are summarized in Table 1. The ORTEP plot of the ligand is depicted in Figure 4, and selected bond distances and bond angles are presented in Table 2 and 3, respectively.

Table 1. Crystal data and structure refinement for $N(SO_2bip)dpa$.

Crystal data	$N(SO_2bip)dpa$
Empirical formula	$C_{24}H_{21}N_3O_2S$
Mr	415.50
Crystal description	Plate, colourless
Crystal system	Triclinic
Space group	P-1
Crystal size (mm)	$0.32 \times 0.21 \times 0.12$
Temperature (K)	90
Unit cell dimensions:	
a (Å)	5.7237 (2)
b (Å)	12.8021 (5)
c (Å)	14.0544 (6)
α (deg)	96.938 (2)
β (deg)	97.863 (2)
γ (deg)	93.922 (2)
V (Å^3)	1008.90 (7)
Z	2
Radiation wavelength/ (Å)	0.71073
abs coeff (mm^{-1})	0.19
2θmax (deg)	72.8
$R[F^2 > 2\sigma(F^2)]$	0.050
$wR(F^2)$	0.134
res. dens (e Å^{-3})	-0.32, 0.71
data/param	9781/271

The obtained S–N bond length (1.6414(8) Å) of L1 is comparable with the S–N bond lengths of 1.6194(11) Å for *N*(SO₂pip)dpa (Subasinghe 2015), 1.602(9) Å for N-methyltoluene-p-sulfonamide (Häkkinen, Ruostesuo et al. 1988) and 1.641(2) Å for N, N-dimethyltoluene-p-sulfonamide (Häkkinen, Ruostesuo et al. 1988).
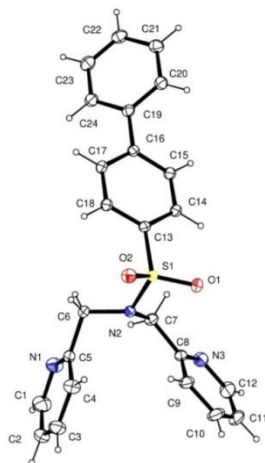

Figure 4. ORTEP plot of *N*(SO₂bip)dpa. Thermal ellipsoids are drawn from 50% probability.

Table 2. Selected bond distances (Å) for *N*(SO₂bip)dpa.

	Bond length (Å)		**Bond length (Å)**
S1 — O1	1.4344 (7)	N3 — C12	1.3457 (17)
S1 — O2	1.4353 (8)	C5 — C6	1.5105 (13)
S1 — N2	1.6414 (8)	C7 — C8	1.5112 (14)
S1 — C13	1.7621 (11)	C16 — C19	1.4787 (14)
N2 — C6	1.4820 (11)	C13 — C14	1.3942 (14)
N2 — C7	1.4717 (13)	C13 — C18	1.3981 (13)
N1 — C1	1.3474 (15)	C4 — C5	1.3853 (16)
N1 — C5	1.3373 (13)	C8 — C9	1.3873 (16)
N3 — C8	1.3414 (14)	C16 — C17	1.4044 (14)

Table 3. Selected bond angles (deg) for *N(*SO$_2$bip)dpa.

	Bond angle (deg)		Bond angle (deg)
O1 — S1 — O2	120.19 (5)	C4 — C5 — C6	120.50 (9)
O1 — S1 — N2	106.10 (4)	N2 — C6 — C5	108.97 (8)
O2 — S1 — N2	106.81 (4)	N2 — C6 — H6A	108.3
O1 — S1 — C13	108.10 (4)	N2 — C7 — C8	114.43 (9)
O2 — S1 — C13	108.17 (5)	N2 — C7 — H7A	108.7
C5 — N1 — C1	116.90 (11)	C8 — C7 — H7A	108.7
C7 — N2 — C6	115.27 (8)	N2 — C7 — H7B	108.7
C7 — N2 — S1	115.78 (6)	C8 — C7 — H7B	108.7
C6 — N2 — S1	117.70 (7)	H7A — C7 — H7B	107.6
C8 — N3 — C12	117.27 (12)	N3 — C8 — C9	123.21 (10)
N1 — C1 — C2	124.46 (11)	N3 — C8 — C7	113.17 (10)
C5 — C4 — C3	119.03 (11)	C9 — C8 — C7	123.63 (10)
C5 — C4 — H4	120.5	C8 — C9 — C10	118.27 (11)
N1 — C5 — C4	122.76 (10)	C14 — C13 — S1	119.61 (8)
N1 — C5 — C6	116.74 (10)	C18 — C13 — S1	119.83 (8)

3.1.3. FTIR Analysis

In an ATR–FTIR spectrum of *N(*SO$_2$bip)dpa (L1), the short absorption band at 3061 cm^{-1} represents the asymmetric stretching vibrations of C–H bonds in aromatic rings, whereas the short absorption peak at 2975 cm^{-1} is attributed to the C–H symmetric stretching vibrations in aliphatic systems (Socrates 2004). The sharp, strong peaks at 1344 cm^{-1} and 1160 cm^{-1} were assigned as the asymmetric and symmetric stretching vibrations of the SO$_2$ group (Roges 1994, Chohan, Youssoufi et al. 2010) and the sharp, strong peak at 923 cm^{-1} was assigned to the S–N stretching vibration (Dardouri, Amor et al. 2015) in the newly synthesized L1. Apart from most ligand peaks which also appear in a spectrum of [Re(CO)$_3$[*N(*SO$_2$bip)dpa]PF$_6$ (C1), two strong and intense absorption peaks at 2038 cm^{-1} and 1908 cm^{-1} due to the stretching vibrations of CO ligands in Re(CO)$_3$ core were observed (Nakamoto 1986). Since lowering of initial bond energy due to the donation of long pair on sp^2 hybridized sulfonamide nitrogen, S–N stretching vibration has shifted to a lower frequency (Table 4).

113

_____

In an ATR-FTIR spectrum of N(SO$_2$bip)dienH (L2) ligand, the small but strong peaks at 2935 cm^{-1} and 2856 cm^{-1} can be assigned to aliphatic C–H stretching vibrations. Peaks at 1328 cm^{-1} and 1162 cm^{-1} were assigned to the asymmetric and symmetric stretching vibrations of SO$_2$. The peak at 943 cm^{-1} was identified as the S–N stretching vibration. It should be noted that stretching vibrations of S–N in a spectrum of [Re(CO)$_3$(N(SO$_2$bip)dien)] have been shifted about 25 cm^{-1} towards higher frequencies (Table 4) due to the effect of deprotonation and the changing of the coordination environment (Darshani, Fronczek et al. 2020). The two strong and sharp absorption peaks at 2005 cm^{-1} and 1861 cm^{-1} are attributed to the stretching vibrations of CO ligands in [Re(CO)$_3$]$^{+}$ core (Nakamoto 1986, Socrates 2004, Bulut, Öztürk et al. 2015).

Table 4: Selected IR bands/cm^{-1} of N(SO2bip)dpa (L1), [Re(CO)$_3$[N(SO$_2$bip)dpa]PF$_6$ (C1), N(SO$_2$bip)dienH (L2), [Re(CO)$_3$(N(SO$_2$bip)dien)] (C2).

Ligand/Complex	νS-N	ν_{as}(SO$_2$)	ν_s(SO$_2$)	ν(CO)
L1	923	1344	1160	
C1	821	1368	1172	2038, 1908
L2	943	1328	1162	
C2	968	1276	1128	2005,1861

3.1.4. UV visible analysis

The peaks that are observed for the UV-visible absorption spectra of ligands and complexes were assigned, focusing on the theoretical background of UV-visible spectroscopy and corresponding literary reported data of the related compounds. The electronic spectra of N(SO$_2$bip)dpa (L1) and [Re(CO)$_3$[N(SO$_2$bip)dpa]PF$_6$ (C1) were recorded in methanol (Figure 5). Two peaks were visible in the spectrum of L1; the peak at 211 nm due to inter-ligand n→π* transition and a less intense low energy absorption peak at 266 nm due to intraligand π→π* transition (Raszeja 2012).
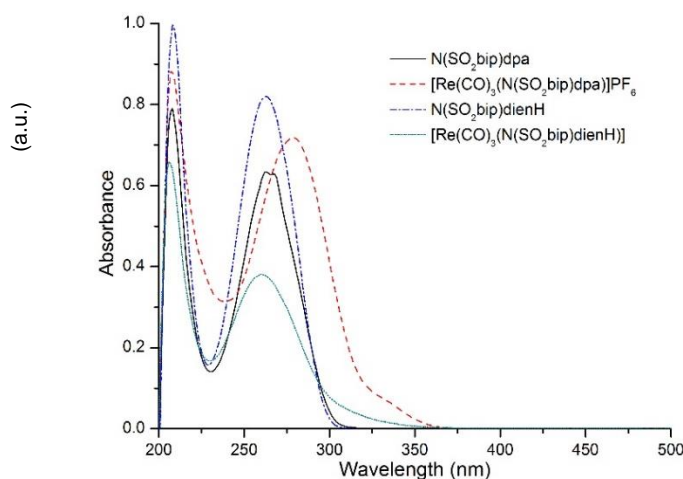

Figure 5. UV visible spectrum of 0.1 mM solution of N(SO$_2$bip)dpa, [Re(CO)$_3$[N(SO$_2$bip)dpa]PF$_6$, N(SO$_2$bip)dienH and [Re(CO)$_3$(N(SO$_2$bip)dien)] in methanol

For the C1 complex, two absorption peaks observed at 207 nm and 275 nm are attributed to ligand centered n→π* and π→π* transitions, respectively upon coordination of ligand to Re(I). The extent of the aromatic π system may govern the energy of the transitions in N(SO$_2$bip)dpa, resulting intraligand transitions (Raszeja 2012). The increase in transition wavelength is observable in the π→π* transition of the complex compared to that of the free ligand, resulting in a bathochromic shift due to the stabilization of π* orbitals more than π orbitals by polar solvent like methanol, leading to a net decrease in transition energy.

The absorption spectra of N(SO$_2$bip)dienH (L2) and [Re(CO)$_3$(N(SO$_2$bip)dien)] (C2) (Figure 5) were measured in methanol at room temperature. The uncoordinated ligand shows two absorption peaks at 208 nm and 260 nm which can be assigned for intraligand n→π* and π→π* transitions, respectively. The absorption spectrum of C2 also displays ligands centered n→π* transition at 206 nm and π→π* transition band at 250 nm. The spectrum of the L2 has shifted towards a shorter wavelength resulting in a hypsochromic shift. The absorption intensity of C2 has decreased in comparison to L2 (Raszeja 2012).

3.1.5. Fluorometric analysis

Fluorescence spectra were obtained for N(SO$_2$bip)dpa (L1) and [Re(CO)$_3$(N(SO$_2$bip)dpa)]PF$_6$ (C1) in methanol. The concentration of the test samples was 0.01 mol/dm^3. Relevant emission details are summarized in Table 5.

Table 5. Excitation and emission wavelengths of N(SO$_2$bip)dpa and [Re(CO)$_3$(N(SO$_2$bip)dpa)]PF$_6$ in methanol.

Test sample	Excitation wavelength /nm	Emission wavelength /nm
N(SO$_2$bip)dpa	350	430
[Re(CO)$_3$(N(SO$_2$bip)dpa)]PF$_6$	350	424

The emissions observed for L1 may occur due to the π→π* and n→π* transitions. However, both ligand and complex show moderate fluorescence intensity, and the decrease in the fluorescence intensity of the C1 compared with L1 may be attributed to the quenching of fluorescence upon direct binding of sulfonamide nitrogen to rhenium.

3.2. Biological studies

3.2.1. Prediction of drug-likeness

Drug likeliness scores built on Lipinski's "rule of five" states that an orally active drug ideally should contain a molecular weight under 500 g/mol, logP less than 5, less than 5 hydrogen bond donors, less than 10 hydrogen bond acceptors, less than 150 topological polar surface area and less than 10 rotatable bonds (Khan, Malla et al. 2017). *In-silico* studies revealed that the two ligands L1 and L2 agree with drug-likeliness analysis with no violations (Table 6).

Table 6. Virtual screening of ligands for drug-likeness estimated using Molinspiration, Molsoft and ChemAxon servers.

	$N(SO_2bip)dpa$	$N(SO_2bip)dienH$
miLogP	3.50	1.04
TPSA	63.16	84.22
natoms	30	22
MW	415.52	319.43
nON	5	5
nOHNH	0	4
nviolations	0	0
nrotb	7	8
volume	367.77	290.18
Molar mass (g/mol)	415.51	319.42
LogP	3.96	1.40
Polar surface area (Å^2)	50.16	74.71
H bond donors	0	4
H bond acceptors	5	5
Lipinski's rule of 5	✓	✓

3.2.2. In vitro cytotoxic effects

The cytotoxic activity of compounds towards the NCI-H292 cell line was analyzed for all four new compounds where they were exposed to the compounds in a concentration gradient. Half maximal inhibitory concentration (IC_{50}) was determined for each compound at 24 h, 48 h and 72 h (Table 7).

Table 7. IC$_{50}$ values reported for ligands and the complexes at 24, 48, and 72 h incubation period.

Test compound	IC$_{50}$ values /µM		
	24 h	48 h	72 h
N(SO$_2$bip)dpa (L1)	52.85	13.91	18.25
[Re(CO)$_3$[*N*(SO$_2$bip)dpa]PF$_6$ (C1)	97.72	35.84	110.93
N(SO$_2$bip)dienH (L2)	16.65	10.05	2.37
[Re(CO)$_3$(*N*(SO$_2$bip)dien)] (C2)	39.91	10.25	15.47

Both the ligands and complexes display significant cytotoxicity towards NCI-H292 cells at low concentrations. The lower concentration of the drugs is desirable for cancer treatment to prevent the occurrence of side effects. Cisplatin is used in chemotherapy against lung cancer and in research as a standard to compare the potency of drug leads. Values obtained for the ligands and Re complexes are comparable to or better than the reported IC$_{50}$ of cisplatin against NCI-H292(Table 8). Furthermore, IC$_{50}$ value of *N*(SO$_2$bip)dpa (L1) has reduced 3.7 folds after 48 h compared to the value obtained at 24 h, whereas [Re(CO)$_3$(*N*(SO$_2$bip)dpa)]PF$_6$ (C1) treatment resulted in a reduction of only 2.7 folds. Interestingly, the cells treated with C1 demonstrate recovery over time where the values have increased beyond the value obtained at 24 h. Rapid revival of proliferation is undesirable for a chemotherapeutic agent, but sustained cytotoxicity is a sign of potency for L1 to be considered as a lead compound in anticancer drug development. All four compounds (L1, L2, C1 and C2) have shown cytocidal and cytostatic effects and can be further tested to develop them as anticancer drug leads. Here we observe that Re complexes are ~2 fold lower in its activity compared to their ligands. However, we have previously demonstrated that in a similar system, N(SO$_2$)(1-nap)dienH ligand showing 12 fold lower activity than its Re(CO)$_3$ derivative (Darshani, Fronczek et al. 2020). In a similar study we have observed that there is no significant cytotoxicity displayed by N(SO$_2$)(1-nap)dpa and its Re(CO)$_3$ derivative (Darshani, Thushara et al. 2020). It is noteworthy that there are contrasting effects exerted upon minor structural changes in this system; hence exploring a range of ligands and compounds with biological systems can yield potential drug leads similar to what is reported here for further exploration.

Table 8. IC$_{50}$ value comparison for ligands and the complexes with cisplatin at 24 hrs incubation period. * according to https://www.cancerrxgene.org accessed on 06/25/2022.

Compound	IC$_{50}$/ µM	Comparative activity
Cisplatin	88.18*	-
N(SO$_2$bip)dpa	52.85	1.7x
[Re(CO)$_3$(N(SO$_2$bip)dpa)]$^+$	97.72	0.9x
N(SO$_2$bip)dienH	16.65	5.3x
[Re(CO)$_3$(N(SO$_2$bip)dien)]	39.91	2.2x

4. Conclusion

Two novel rhenium tricarbonyl complexes, C1 and C2, with pendant biphenyl groups were synthesized and characterized by various spectroscopies methods. L1 was further characterized by single crystal X-ray diffraction. Both L1 and L2 are in compliance with calculated drug likeliness scores that indicate their potential applicability as drug leads. A preliminary study carried out to assess the in vitro cytotoxicity of these compounds on lung cancer cell line NCI-H292 revealed that all four compounds, L1, L2, C1 and C2 displayed significant cytotoxic activity. IC50 values obtained for L2,were the lowest out of all four compounds and decreased with increasing incubation time which leads us to propose that L2, in particular, exhibits a promising characteristic for an anticancer drug lead.

Competing interests

The authors declare that they have no competing interests.

References

Abhayawardhana, P. L., Marzilli, P. A., Fronczek, F. R. and Marzilli, L. G. (2014). "Complexes possessing rare "tertiary" sulfonamide nitrogen-to-metal bonds of normal length: *fac*-[Re (CO)$_3$(N (SO$_2$R) dien)]PF$_6$ complexes with hydrophilic sulfonamide ligands." Inorganic Chemistry **53**(2): 1144-1155.

Amoroso, A. J., Coogan, M. P., Dunne, J. E. , Fernández-Moreira, V., Hess, J. B. , Hayes, A. J., Lloyd, D., Millet, C., Pope, S. J. and Williams, C. (2007). "Rhenium fac tricarbonyl bisimine complexes: biologically useful fluorochromes for cell imaging applications." Chemical Communications (29): 3066-3068.

Arnott, J. A. and Planey, S. L. (2012). "The influence of lipophilicity in drug discovery and design." Expert Opinion on Drug Discovery **7**(10): 863-875.

Atkins, P., Overton, T., Rourke, J., Weller, M. and Armstrong, F. S. (2006). Atkins' inorganic Chemistry, Oxford University Press: Oxford, UK.

Banerjee, S. R., Levadala, M. K., Lazarova, N. , Wei, L. , Valliant, J. F., Stephenson, K. A. , Babich, J. W. , Maresca, K. P. and Zubieta, J. (2002). "Bifunctional Single Amino Acid Chelates for

Labeling of Biomolecules with the $\{Tc(CO)_3\}^+$ and $\{Re(CO)_3\}^+$ Cores. Crystal and Molecular Structures of [ReBr (CO)$_3$(H$_2$NCH$_2$C$_5$H$_4$N)],[Re(CO)$_3$\{(C$_5$H$_4$NCH$_2$)$_2$NH\}]Br, [Re(CO)$_3$\{(C$_5$H$_4$NCH$_2$)$_2$NCH$_2$CO$_2$H\}]Br, [Re(CO)$_3$\{X (Y)NCH$_2$CO$_2$CH$_2$CH$_3$\}]Br (X= Y= 2-pyridylmethyl; X= 2-pyridylmethyl, Y= 2-(1-methylimidazolyl) methyl; X= Y= 2-(1-methylimidazolyl) methyl),[ReBr(CO)$_3$\{(C$_5$H$_4$NCH$_2$)NH(CH$_2$C$_4$H$_3$S)\}], and [Re(CO)$_3$\{(C$_5$H$_4$NCH$_2$)N(CH$_2$C$_4$H$_3$S)(CH$_2$CO$_2$)\}]." Inorganic Chemistry **41**(24): 6417-6425.

Bulut, I., Öztürk, F. and Bulut, A. (2015). "Synthesis, structural and electrochemical properties of nickel (II) sulfamethazine complex with diethylenetriamine ligand." Spectrochimica Acta Part A: Molecular and Biomolecular Spectroscopy **138**: 138-145.

Chohan, Z. H., Youssoufi, M. H., Jarrahpour, A. and Haddia, T. B. (2010). "Identification of antibacterial and antifungal pharmacophore sites for potent bacteria and fungal inhibition of indolenyl sulfonamide derivatives." European Journal of Medicinal Chemistry **45**: 1189-1199.

Christoforou, A. M., Marzilli, P. A., Fronczek, F. R. and Marzilli, L. G. (2007). "*fac*-[Re(CO)$_3$L]$^+$ Complexes with N-CH$_2$-CH$_2$-X-CH$_2$-CH$_2$-N Tridentate Ligands. Synthetic, X-ray Crystallographic, and NMR Spectroscopic Investigations." Inorganic Chemistry **46**(26): 11173-11182.

Cleare, M. J. and Hoeschele, J. D. (1973). "Studies on the antitumor activity of group VIII transition metal complexes. Part I. Platinum (II) complexes." Bioinorganic Chemistry **2**(3): 187-210.

Dardouri, M., A. , Amor, H. and Meganem, F. (2015). "Preparation, characterization and ion adsorption properties of functionalized polystyrene modified with 1, 4-phenylene diisocyanate and diethylenetriamine." Chemical Papers **69**(12): 1617-1624.

Darshani, T., Fronczek, F. R. , Priyadarshani, V. V. , Samarakoon, S. R. , Perera, I. C. and Perera, T. (2020). "Synthesis and characterization of novel naphthalene-derivatized tridentate ligands and their net neutral rhenium tricarbonyl complexes and cytotoxic effects on non-small cell lung cancer cells of interest." Polyhedron **187**: 114652.

Darshani, T., Thushara, N. , Weerasuriya, P. , Fronczek, F. R., Perera, I. C. and Perera, T. (2020). "Fluorescent di-(2-picolyl)amine based drug-like ligands and their Re(CO)$_3$ complexes towards biological applications." Polyhedron **185**: 114592.

Desbouis, D., Struthers, H. , Spiwok, V. , Küster, T. and Schibli, R. (2008). "Synthesis, *in vitro*, and *in silico* evaluation of organometallic technetium and rhenium thymidine complexes with retained substrate activity toward human thymidine kinase type 1." Journal of Medicinal Chemistry **51**(21): 6689-6698.

Fulmer, G. R., Miller, A. J., Sherden, N. H. , Gottlieb, H. E. , Nudelman, A. , Stoltz, B. M. , Bercaw, J. E. and Goldberg, K. I. (2010). "NMR chemical shifts of trace impurities: common laboratory solvents, organics, and gases in deuterated solvents relevant to the organometallic chemist." Organometallics **29**(9): 2176-2179.

Garcia, M., Jemal, A. , Ward, E. , Center, M. , Hao, Y. , Siegel, R. and Thun, M. (2007). "Global cancer facts & figures 2007." Atlanta, GA: American Cancer Society **1**(3): 52.

Häkkinen, A.-M., Ruostesuo, P. and Kivekäs, R. (1988). "Nuclear magnetic resonance and X-ray diffraction studies on some substituted benzenesulphonamides." Journal of the Chemical Society, Perkin Transactions 2(6): 815-820.

He, H., Lipowska, M. , Xu, X. , Taylor, A. T., Carlone, M. and Marzilli, L. G. (2005). "Re (CO)$_3$ Complexes Synthesized via an Improved Preparation of Aqueous *fac*-[Re(CO)$_3$(H$_2$O)$_3$]+ as an Aid in Assessing ^{99m}Tc Imaging Agents. Structural Characterization and Solution Behavior of

119

_____

Complexes with Thioether-Bearing Amino Acids as Tridentate Ligands." Inorganic Chemistry **44**(15): 5437-5446.

Kadi, A. A., El-Brollosy, N. R., Al-Deeb, O. A., Habib, E. E. , Ibrahim, T. M. and El-Emam, A. A. (2007). "Synthesis, antimicrobial, and anti-inflammatory activities of novel 2-(1-adamantyl)-5-substituted-1, 3, 4-oxadiazoles and 2-(1-adamantylamino)-5-substituted-1, 3, 4-thiadiazoles." European Journal of Medicinal Chemistry **42**(2): 235-242.

Khan, S., Malla, A. M. , Zafar, A. and Naseem, I. (2017). "Synthesis of novel coumarin nucleus-based DPA drug-like molecular entity: In vitro DNA/Cu (II) binding, DNA cleavage and pro-oxidant mechanism for anticancer action." PloS one **12**(8): e0181783.

KK-W, L., C. AW-T and L. WH-T (2012). "Applications of luminescent inorganic and organometallic transition metal complexes as biomolecular and cellular probes." Dalton Transactions **41**(20): 6021-6047.

KK-W., L. (2015). "Luminescent rhenium (I) and iridium (III) polypyridine complexes as biological probes, imaging reagents, and photocytotoxic agents." Accounts of Chemical Research **48**(12): 2985-2995.

Kunnumakkara, A. B., Bordoloi, D. , Sailo, B. L., Roy, N. K., Thakur, K. K., Banik, K. , Shakibaei, M. , Gupta, S. C. and Aggarwal, B. B. (2019). "Cancer drug development: The missing links." Experimental Biology and Medicine **244**: 244: 663–689.

Lo, K. K.-W., M.-W. Louie, K.-S. Sze and J. S.-Y. Lau (2008). "Rhenium (I) polypyridine biotin isothiocyanate complexes as the first luminescent biotinylation reagents: synthesis, photophysical properties, biological labeling, cytotoxicity, and imaging studies." Inorganic Chemistry **47**(2): 602-611.

Lo, K. K. W., Zhang, K. Y. and Li, S. P. Y. (2011). "Recent exploitation of luminescent rhenium (I) tricarbonyl polypyridine complexes as biomolecular and cellular probes." European Journal of Inorganic Chemistry **2011**(24): 3551-3568.

Nakamoto, K. (1986). Infrared and Raman spectra of inorganic and coordination compounds, Wiley Online Library.

Perera, T., Abhayawardhana, P. , Marzilli, P. A., Fronczek, F. R. and Marzilli, L. G. (2013). "Formation of a metal-to-nitrogen bond of normal length by a neutral sufonamide group within a tridentate ligand. A new approach to radiopharmaceutical bioconjugation." Inorganic Chemistry **52**(5): 2412-2421.

Pizarro, A. M. and Sadler, P. J. (2009). "Unusual DNA binding modes for metal anticancer complexes." Biochimie **91**(10): 1198-1211.

Raszeja, M. S. L. (2012). "Luminescent Phenanthridinyl-Containing Rhenium Tricarbonyl Complexes About Cellular Imaging, Biological Activity and Functional Labels for Peptide Nucleic Acids and Peptides."

Roges, N. P. G., Ed. (1994). A guide to the complete interpretatation of the infra red spectra of organic structures. New York, Wiley.

Rutkowska, E., Pajak, K. and Jóźwiak, K. (2012). "Lipophilicity--methods of determination and its role in medicinal chemistry." Acta Poloniae Pharmaceutica **70**(1): 3-18.

Schibli, R. and Schubiger, A. P. (2002). "Current use and future potential of organometallic radiopharmaceuticals." European Journal of Nuclear Medicine and Molecular Imaging **29**(11): 1529-1542.

Schibli, R., Schwarzbach, R. , Alberto, R. , Ortner, K. , Schmalle, H. , Dumas, C. , Egli, A. and Schubiger, P. A. (2002). "Steps toward high specific activity labeling of biomolecules for therapeutic application: preparation of precursor $[^{188}Re(H_2O)_3(CO)_3]^+$ and synthesis of tailor-made bifunctional ligand systems." Bioconjugate Chemistry **13**(4): 750-756.

Scozzafava, A., Owa, T. , Mastrolorenzo, A. and Supuran, C. T. (2003). "Anticancer and antiviral sulfonamides." Current Medicinal Chemistry **10**(11): 925-953.

Socrates, G. (2004). Infrared and Raman characteristic group frequencies: tables and charts, John Wiley & Sons.

Subasinghe, S. A. A. S. (2015). "Synthesis Characterization and Biological Studies of Piperidinyl Apended Dipicolylamine Rhenium Tricarbonyl Complexes as Potential Diagnostic Agents." Bioinorganic Chemistry and Applications

Testa, B., Crivori, P. , Reist, M. and Carrupt, P.-A. (2000). "The influence of lipophilicity on the pharmacokinetic behavior of drugs: Concepts and examples." Perspectives in Drug Discovery and Design **19**(1): 179-211.

Vitharana, N. V., Kaushalya, C. , Perera, T. , Deraniyagala, S. P. , Sameera, W. M. C. and Cooray, A. T. "Dipicolylamine based fluorescent probes for determination of Fe^{3+}: Analytical and theoretical aspects" Accepted ACS Omega 2022.

Wolf, I., O'Kelly, J., Wakimoto, N. , Nguyen, A. , Amblard, F. , Karlan, B. Y., Arbiser, J. L. and Koeffler, H. P. (2007). "Honokiol, a natural biphenyl, inhibits in vitro and in vivo growth of breast cancer through induction of apoptosis and cell cycle arrest." International Journal of Oncology **30**(6): 1529-1537.